© August 2026 | IJIRT | Volume 13 Issue 3 | ISSN: 2349-6002

Effect Of Wind on Soil-Structure Interaction: A Study on Hoarding Structure

Sahil Abdulgani Shaikh
M.Tech Student, Department of Civil Engineering
G H Raisoni College of Engineering and Management, Pune, India

Abstract—Hoarding structures are tall, wind sensitive lattice structures carried on a slender mast with a comparatively small foundation footprint, and are conventionally analysed assuming a rigid, fixed base support, an assumption that ignores the flexibility of the founding soil. This study evaluates the effect of Soil Structure Interaction (SSI) on a 19-metre wide, about 18-metre-tall lattice hoarding supported on a 4 column Circular Hollow Section (CHS) mast, by comparing a conventional fixed base STAAD.Pro model against a spring supported model in which the footing stiffness is represented explicitly using the NIST GCR 12-917-21 and Pais-Kausel embedded footing impedance method. The founding soil, a silty sand with governing SPT N value of 13, was assessed per IS 6403 for a 6.7 metre square footing at 2.0 metre embedment. The results show that allowing the footing to translate and rotate redistributes load away from the axial force couple between legs, with maximum leg compression falling by 57 percent and maximum uplift by 66 percent relative to the fixed base case, while the governing leg moment rises by 204 percent. An independent ETABS check confirms the top of mast displacement more than doubles under the spring supported condition. The base plate and RCC pedestal, designed for the conservative fixed base reactions, are both found adequate, with the manual pedestal design corroborated by an independent RCDC check within one percentage point.

Index Terms—bearing capacity, ETABS, foundation stiffness, hoarding structure, RCDC, soil-structure interaction, STAAD. Pro, wind load

I. INTRODUCTION

Hoarding structures, large outdoor advertisement panels mounted on a slender supporting mast, are widely used along highways and urban roads. Structurally, a hoarding behaves as a cantilevered lattice frame: a wide, relatively lightweight panel exposed to a large wind catching area, carried on a comparatively slender steel mast and a small footprint foundation. This combination makes wind, not gravity load, the governing action in the design of both the superstructure and the foundation.

Conventional structural analysis of such systems almost always assumes a fixed base, where the foundation is treated as an infinitely rigid support that permits no translation or rotation. In reality, the soil beneath the footing is a deformable medium, and under the large overturning moments that wind generates on a tall, slender hoarding, the footing can translate and rotate measurably. Representing this flexibility explicitly, an approach broadly termed Soil-Structure Interaction (SSI), changes both the distribution of internal forces in the structure and the deflection at the top of the mast. This paper studies a specific, fully detailed hoarding structure sited in Pune, Maharashtra, a 19-metre wide, about 18-metre-tall lattice panel on a 4 column CHS mast, and compares its response under a conventional fixed base STAAD.Pro model against a spring supported model in which the footing stiffness is derived from first principles using a recognised geotechnical impedance method. Fig. 1 shows the overall elevation of the structure with its key dimensions.

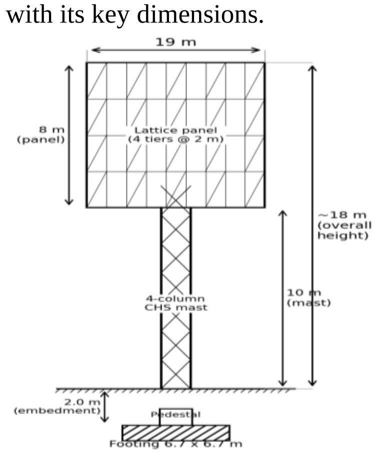

Fig. 1. Elevation of the hoarding structure showing overall dimensions.

II. LITERATURE REVIEW

Wind loading on sign and billboard type structures has long been recognised as the governing design action [9], [10], [11], with force coefficients found to vary with panel elevation and design code. The static and dynamic stiffness formulations of Gazetas [8] and the embedded footing impedance functions of Pais and Kausel [7], later adopted with embedment corrections in NIST GCR 12-917-21 [6], remain the standard reference for converting footing geometry and soil properties into translational and rotational spring constants. Reviews of SSI applied to slender, wind or dynamically loaded structures such as lattice transmission towers [14] and wind turbine towers [15], [16] consistently report that neglecting foundation flexibility changes the base force distribution and the top displacement relative to a fixed base idealisation [17].

Separately, the assessment of shallow foundation bearing capacity from Standard Penetration Test data via IS 6403 [1] is a mature, widely validated method in Indian geotechnical practice [18]. Published work combining all three strands into a full comparative fixed base versus spring supported study is limited, and this is the gap addressed here.

III. METHODOLOGY

A. Bearing Capacity Assessment

The founding soil, a silty sand at the project site (18.52 degrees N, 73.85 degrees E), was assessed per IS 6403:1981 using the Standard Penetration Test value from bore hole BH-1 (governing SPT-1, N = 13, at 2.00 to 2.45 m depth). After overburden and dilatancy corrections, the corrected value N2 = 21 gives an angle of shearing resistance of approximately 33 degrees.

The net ultimate bearing capacity is given by (1).

$$q_d = q(N_q - 1)\, s_q\, d_q\, i_q + 0.5\, B\, \gamma\, N_\gamma\, s_\gamma\, d_\gamma\, i_\gamma\, W' \quad (1)$$

where q is the effective surcharge, N_q and N_γ are bearing capacity factors, s, d and i are the shape, depth and inclination correction factors, and W' is the water table correction factor. For the 6.7 m square footing at 2.0 m embedment, this gives a net safe bearing capacity of 864.2 kPa and a gross safe bearing capacity of 900.2 kPa at a factor of safety of 2.5.

B. Soil Spring Stiffness Calculation

Soil spring stiffness was derived using the NIST GCR 12-917-21 and Pais-Kausel embedded footing impedance method. Fig. 2 shows the lumped mass idealisation used: the structure is represented as a mass m on the mast stiffness k, and the flexible footing is represented by three independent springs at its centre, Kx for horizontal translation, Kz for vertical translation, and Kyy for rocking.

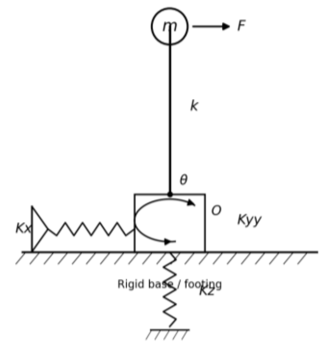

Fig. 2. Lumped-mass model with three soil springs at the base.

The static surface stiffness in the vertical direction is given by (2).

$$K_{z,sur} = [2GL / (1 - \nu)]\, [0.73 + 1.54(B/L)^{0.75}] \quad (2)$$

where G is the soil shear modulus, L and B are the footing half length and half width, and ν is the soil Poisson's ratio.

Each surface stiffness is then corrected for embedment depth using (3).

$$K = K_{sur} \times \eta \quad (3)$$

where η is an embedment correction factor. This method gives a vertical stiffness Kz of 500,498 kN/m, a horizontal stiffness Kx of 510,130 kN/m, and a rocking stiffness Kyy of 6,987,684 kN.m/rad. A dynamic modifier check confirms the wind loading condition is quasi static, so no dynamic reduction of these stiffness values is required.

C. STAAD.Pro Modelling

The hoarding structure was modelled in STAAD.Pro 2025 under two support conditions using an identical set of IS 875 (Part 3) based wind load combinations: a conventional fixed base model, with all six degrees of freedom restrained at each of the four leg nodes, and a spring supported model, with the stiffness values from Section III-B applied at each leg node.

D. Design of Base Plate and RCC Pedestal

The common base plate and its 60-anchor bolt group (M36 Grade 8.8, 15 bolts per leg in an independent square ring around each column) were designed for the governing fixed base reactions using the elastic bolt group method.

The RCC pedestal below the base plate was designed using a strain compatibility method per IS 456, and independently verified using RCDC linked directly to the STAAD analysis file.

IV. STRUCTURAL DETAILS OF THE HOARDING

The structure is a lattice frame hoarding, 19 m wide and approximately 18 m tall overall (8 m panel depth on a 10 m mast), supported on 4 legs of CHS 609.6 mm outer diameter by 20 mm wall thickness, arranged on a 2 by 2 grid at 1000 mm centres. TABLE I summarises the key structural parameters.

TABLE I KEY STRUCTURAL PARAMETERS

Parameter	Value
Panel width	19 m
Overall height	~18 m
Leg section	CHS 609.6 x 20 mm
Leg spacing (c/c)	1000 mm
Footing size	6.7 x 6.7 x 0.85 m
Embedment depth	2.0 m
Base plate	1900 x 1900 x 50 mm
Anchor bolts	60 nos. M36 Gr 8.8
Pedestal	2200 x 2200 x 1200 mm

V. RESULTS AND DISCUSSION

A. Bearing Capacity and Spring Stiffness

The IS 6403 assessment gives a net safe bearing capacity of 864.2 kPa and gross safe bearing capacity of 900.2 kPa. The NIST GCR 12-917-21 and Pais-Kausel method gives embedded soil spring stiffness of Kz = 500,498 kN/m, Kx = 510,130 kN/m and Kyy = 6,987,684 kN.m/rad for the same footing.

B. Comparative Structural Response

TABLE II compares the governing reactions under load combination 1.5(DL+WL) between the fixed base and spring supported models. Allowing the footing to translate and rotate redistributes load away from the axial force couple between legs: maximum leg compression falls by 57 percent and maximum uplift by 66 percent relative to the fixed base case. The same flexibility shifts demand into local bending at each support instead, with the governing leg moment rising by 204 percent. Fig. 3 illustrates this redistribution graphically.

TABLE II COMPARATIVE STRUCTURAL RESPONSE (LOAD 4 GOVERNING)

Quantity	Fixed Base	Spring-Supp.	Change
Max compression (kN)	2376.4	1016.2	-57%
Max uplift (kN)	-2070.5	-710.2	-66%
Max leg moment (kN.m)	333.0	1011.6	+204%
Wind base shear (kN)	277.2	277.2	0%

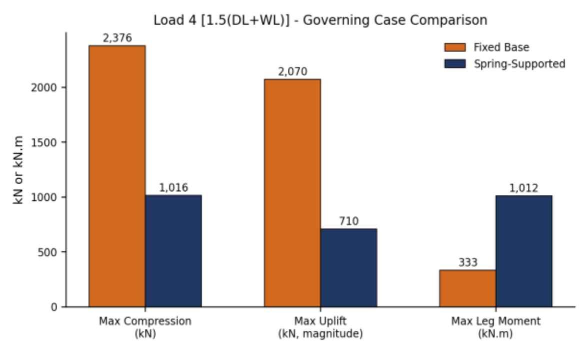

Fig. 3. Comparison of fixed-base and spring-supported governing response.

C. Deflection Comparison

TABLE III compares the top of mast deflection and other displacement quantities. Rocking stiffness dominates the SSI response, contributing an additional 14.9 to 30.0 mm of top sway analytically, against settlement and sliding of only 1.2 mm and 0.8 mm respectively.

An independent ETABS check corroborates this shift, with the maximum top of mast displacement more than doubling under the spring supported condition, from 115.47 mm to 250.39 mm, an increase of 117 percent.

TABLE III DEFLECTION COMPARISON

Quantity	Fixed Base	Spring-Supp.
Max top displacement (ETABS)	115.47 mm	250.39 mm
Additional sway from rocking	-	14.9-30.0 mm
Settlement under P total	-	1.22 mm
Sliding under V total	-	0.82 mm

D. Base Plate and Pedestal Design

Fig. 4 shows the anchor bolt layout adopted for the common base plate: each leg carries its own independent ring of 15 bolts, giving 60 bolts (M36 Grade 8.8) in total.

The base plate and RCC pedestal, both designed for the more conservative fixed base reactions, are found adequate with all utilisations below 50 percent: bolt tension utilisation of 47.4 percent, combined shear tension utilisation of 22.5 percent, and pedestal moment capacity utilisation of 34.5 percent.

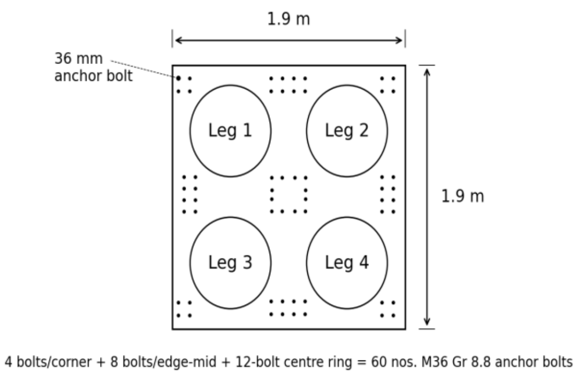

Fig. 4. Common base plate anchor bolt layout (60 nos. M36 bolts).

E. Manual Calculation vs. Software Verification

TABLE IV compares the manual strain compatibility pedestal design against an independent RCDC check. Despite different governing load combinations and assumed concrete grades, the manual and RCDC results converge closely on the capacity utilisation, 34.5 percent manual against 34 percent RCDC, because both are governed by the code minimum reinforcement rather than by demand.

TABLE IV MANUAL VS. SOFTWARE VERIFICATION (RCC PEDESTAL)

Quantity	Manual	RCDC
Design moment (kN.m)	6271.6	5770.7
Moment capacity (kN.m)	18169.9	17117.2
Capacity utilisation	34.5%	34%
Shear stress (MPa)	0.089	0.088

VI. CONCLUSION

This study set out to quantify whether a conventional fixed base analysis misrepresents the structural demand on a wind loaded lattice hoarding relative to a spring supported model. The results confirm that it does: fixed base analysis over predicts axial force demand while under predicting local bending demand and top of mast displacement, by a wide margin in both directions. For this hoarding geometry, designing the base plate and pedestal against the fixed base envelope happens to remain conservative for the axial force driven checks, but the 204 percent increase in leg moment and the 117 percent increase in top displacement under the spring supported condition are large enough that this should not be assumed to hold for every hoarding geometry. SSI based spring modelling is recommended as standard practice for this structure type rather than as an optional refinement.

ACKNOWLEDGMENT

The author thanks the Department of Civil Engineering, G H Raisoni College of Engineering and Management, Pune, for the facilities provided, and Satish Marathe Consulting Engineers for technical support and data access during this study.

REFERENCES

[1] IS 6403:1981, *Code of Practice for Determination of Bearing Capacity of Shallow Foundations*. New Delhi, India: Bureau of Indian Standards, 1981.

[2] IS 875 (Part 3):2015, Code of Practice for Design Loads (Other than Earthquake) for Buildings and

Structures—Part 3: Wind Loads. New Delhi, India: Bureau of Indian Standards, 2015.
[3] IS 800:2007, General Construction in Steel—Code of Practice. New Delhi, India: Bureau of Indian Standards, 2007.
[4] IS 456:2000, Plain and Reinforced Concrete—Code of Practice. New Delhi, India: Bureau of Indian Standards, 2000.
[5] IS 1892:1979, Code of Practice for Subsurface Investigation for Foundations. New Delhi, India: Bureau of Indian Standards, 1979.
[6] National Institute of Standards and Technology (NIST), Soil-Structure Interaction for Building Structures, NIST GCR 12-917-21. Gaithersburg, MD, USA: NEHRP Consultants Joint Venture, 2012.
[7] A. Pais and E. Kausel, "Approximate formulas for dynamic stiffnesses of rigid foundations," Soil Dynamics and Earthquake Engineering, vol. 7, no. 4, pp. 213–227, 1988.
[8] G. Gazetas, "Formulas and charts for impedances of surface and embedded foundations," Journal of Geotechnical Engineering (ASCE), vol. 117, no. 9, pp. 1363–1381, 1991.
[9] C. W. Letchford, "Wind loads on rectangular signboards and hoardings," Journal of Wind Engineering and Industrial Aerodynamics, vol. 89, no. 2, pp. 135–151, 2001.
[10] A. H. J. Al-Rkaby, "Wind design loads on solid signs in Southern Iraq based on different design codes and CFD analysis," research article.
[11] Zhu et al., "Mechanical analysis and model test of large-scale highway billboard under wind load," International Journal of Low-Carbon Technologies, 2025.
[12] "Experimental investigation and estimation of wind load and wind-induced responses of monopole three-sided billboard," Journal of Structural Engineering (ASCE), vol. 148, no. 5, 2022.
[13] "Structural design of signposts and billboards," Structville.
[14] M. Bahari, S. Langlois, and S. Prud'homme, "Determination of the soil-foundation stiffnesses in lattice tower structures for numerical modeling applications," CIGRE Science and Engineering.
[15] "Advancing soil-structure interaction (SSI): A comprehensive review of current practices, challenges, and future directions," Journal of Infrastructure Preservation and Resilience, Springer, 2025.
[16] "Soil-structure interaction: A state-of-the-art review of modeling techniques and studies on seismic response of building structures," Frontiers in Built Environment, 2023.
[17] "Reliability analysis of wind response of flexibly supported tall structures," research article.
[18] "Comparative studies on bearing capacity of shallow foundations from N and φ," Journal of the Institution of Engineers (India): Series A.
[19] K. Terzaghi, Theoretical Soil Mechanics. New York, NY, USA: John Wiley & Sons, 1943.
[20] G. G. Meyerhof, "The ultimate bearing capacity of foundations on slopes," in Proc. 4th Int. Conf. Soil Mechanics and Foundation Engineering, 1957.
[21] J. B. Hansen, "A revised and extended formula for bearing capacity," Danish Geotechnical Institute Bulletin, no. 28, 1970.
[22] W. C. Teng, Foundation Design. Englewood Cliffs, NJ, USA: Prentice-Hall, 1962.